Electrochemical and Computational Studies of Aripiprazole as a Novel Eco-friendly Green Corrosion Inhibitor for Carbon Steel in Aqueous Environment

Mai Mostafa A. Hassan Shanab

Department of Chemistry, Science and Humanity Studies College –Prince Sattam Bin Abdul-Aziz University, P.O. Box: 13 Hawtat Bani Tamim 11149, Saudi Arabia & Forensic and Toxicology Lab., Forensic Medicine, Mansoura, Egypt.
E-mail: m.hassan@psau.edu.sa

The theoretical and experimental study of the corrosion inhibitor of the Expired Aripiprazole drug on carbon steel (CS) in hydrochloric acid corrosive medium (1M) has been examined by employing chemical and electrochemical methods. The inhibition efficiency was found to improve with the rise of the concentration of inhibitor and explained on the basis of adsorption metal surface. The adsorption effect follows Langmuir adsorption isotherm. In the presence and absence of expired Aripiprazole the percent inhibition efficiency (%IE) and activation energy (E_a^*) were calculated. The impact of temperature on corrosion rate was investigated. The morphology of the CS surface was examined using FTIR, AFM, and XPS tests. Results obtain for all methods used are in good agreement. Also, the theoretical calculations were calculated utilizing density functional theory (DFT) and Hartree Fock (HF) method. This electronic molecular parameter of aripiprazole aid to describe the mechanism of prevents CS corrosion. Monte Carlo simulations were also performed to simulate the adsorption of expired aripiprazole drug on iron surface and the results show that ph-N-C=O is the most effective corrosion inhibitor for CS in acidic medium.

1. INTRODUCTION

Whereas, carbon steel is commonly used in a variety of industries, including construction, chemical manufacturing, and oil/gas pipelines, due to its low price and good mechanical properties. All of these properties for CS metal is highly susceptible to attack by acids, especially hydrochloric acid which is known as acid pickling [1][2][3]. It is important to clean the machines with mineral acids, but these acids are aggressive so inhibitors are commonly used to minimize cleaning acid aggressive behavior [4]. To control the process of metallic corrosion, there are several tests, but one of the most

Int. J. Electrochem. Sci., 16 **(2021)** Article Number: 211032

2

significant practical tests used is utilized of corrosion inhibitors in the industrial field as well as in academic studies and inhibit in the literary survey [5][6][7][8]. Corrosion inhibitors are substances that, when added in small amounts to corrosion systems, can reduce or eliminate the interaction of metals with their surroundings. Inhibitors are organic molecules that contain heteroatoms such as nitrogen, oxygen, and sulfur atoms, as well as many bonds, all of which enable them adsorb on the metal's surface and protect it against corrosion [9][10]. It is stated that organic molecules having hetero atoms like O, S, and N are adsorbed on the metal surface by blocking the active center and producing a thin layer, the penetration of corrosive species through the metal is summarized [11].

Aripiprazole is used as a therapeutic of ABILIFY [12], also in the treatment of moderate to severe manic episodes in Bipolar I Disorder and for the prevention of a new manic episode in adults who experienced predominantly manic episodes and schizophrenia [13]. The expired Aripiprazole drug can be disposed of safely as an eco-friendly corrosion inhibitor.

Herein, the study successfully uses the expired Aripiprazole drug as a CS corrosion inhibitor by sharing altered electrons from oxygen and nitrogen atoms to CS. The mechanism of aripiprazole green inhibitor was confirmed theoretically, utilizing WL, electrochemical tests, and surface examinations.

2. EXPERIMENTAL

2.1. Materials and solutions

The hydrochloric acid corrosive media (1 M) was formed by diluting a reagent of analytical grade HCl 37% with bi-distilled water. The applied CS specimens have the following compositions (as Wt. %): C (0.2%), Mn (0.37%), P (0.026%), Si (0.002%) and Fe (rest). The samples of CS were abraded with varying degrees of emery reached 4000 grades, cleaned and washed utilizing acetone and dry with filter paper. The examined expired Aripiprazole was utilized as an inhibitor from Egyptian International Pharmaceutical Industries Company. The structural formulae of expired Aripiprazole are as follows:
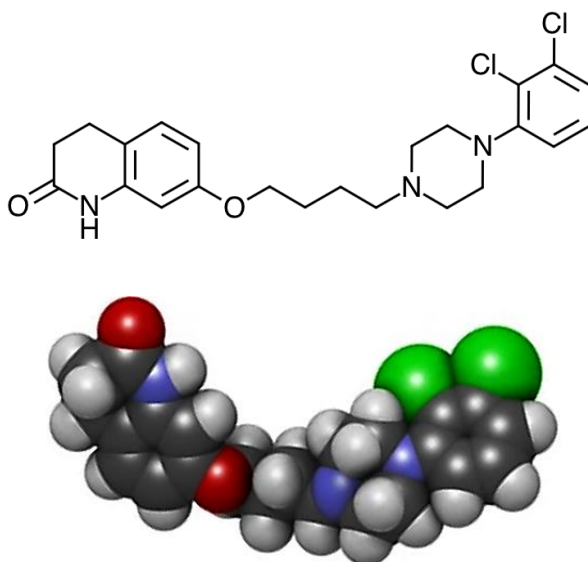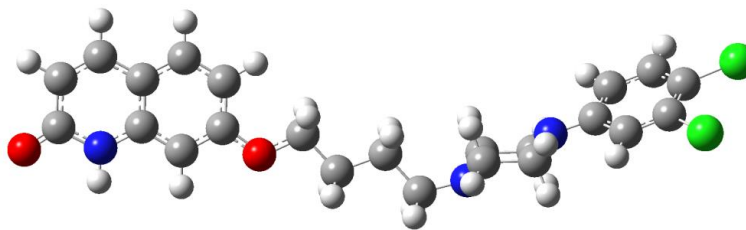
Figure 1. Optimized structure of Aripiprazole ($C_{23}H_{27}Cl_2N_3O_2$) using B3LYP/ 6-31++G(d,p) method, M.wt = 438.39 g/mol

2.2. Weight loss (WL) method

CS samples with sizes 2 x 2 x 0.2 cm were ready as previously. Weighted CS exactly then suspended in solutions of 100 ml of the aggressive environment without and with (50 to 300 ppm) of Aripiprazole for altered immersion time (30, 60, 90, 120, 150 and 180 min). The surface coverage (θ) and % IE were calculated from Eq. (2). The corrosion rate (CR) can be measured as follows:

$$CR = \Delta W/At \qquad (1)$$

Where ΔW is weight loss (mg), A is the area of CS coins in cm^2, and t is the immersion time in min.

2.3. Electrochemical techniques

2.3.1 Potentiodynamic polarization (PP) test

The electrochemical tests were calculated utilizing a Potentiostat / Galvano stat /ZRA. The potentiostat was coupled to a standard cell in the following way: CS metal as the "working electrode (W.E), platinum wire as the counter electrode (C.E), and the Saturated Calomel Electrode (SCE)" as the reference electrode. The experiments began with W.E immersion for thirty minutes in the electrolyte to establish the steady state of the open circuit potential (OCP). The experiment was modified with an electrochemical program on a monitor. The polarization curves were recorded in potential range between - 500 and + 500 mV versus OCP at a scan rate of 1 mVs^{-1}. The corrosion current densities were calculated. The experiments were performed with increasing inhibitor concentrations. The % IE and the level of (θ) were calculated using Eq. (3) [14].

2.3.2 Electrochemical impedance spectroscopy (EIS) test

EIS was calculated after OCP calculation using the identical circuit. The EIS experiments were performed at frequencies from 1 Hz to 100 kHz, with as signal amplitude. %IE and θ from altered chemical and electrochemical measurements were determined as presented in Table (1).

Table 1. The following equation can be used to measure % IE.

Technique	Equation	
WL [12]	% IE = Θ x 100 = **[**1-(W_i / W_0)**]** x100	(2)
PP [13]	%IE= θ × 100 = [1– (i_{corr}/ i^o_{corr})] × 100	(3)
EIS [14]	IE %IE = θ × 100 = [1 – (R^o_{ct}/ R_{ct})] × 100	(4)

Where, W_0 weight loss values without inhibitor, and Wi with it; i_{corr} is the current density with and i^o_{corr} without inhibitor; and a charge transfer resistance values in the absence and presence of the Aripiprazole inhibitor are R^o_{ct}, and R_{ct}, respectively [15].

2.4. Surface examinations

2.4.1 Atomic force microscopy (AFM) analysis

The basic feature of the AFM test is that the surface roughness can be specified. AFM tests were took place using prepared CS specimens before and after immersion for 24 hours in 1 M HCl medium without and with the higher concentration (300 ppm) of the Aripiprazole drug.

2.4.2 Fourier transform infrared spectroscopy (FT-IR) analysis

FT-IR spectra for Aripiprazole before and after adsorption on CS surface. After 24 hours were studied in spectral range 4000 to 500 cm^{-1} with the technique of Attenuated Total Reflectance (ATR) using FTIR-Spectrometer IS 10 (Thermo Fisher Scientific, USA).

2.4.3 X-ray photoelectron spectroscopy (XPS) analysis

The adsorbed atoms and functional groups on the metal surface were deduced utilizing a highly effective system that calculates the binding energies of different bonds found on the CS utilizing (XPS). "XPS analysis was done by K-ALPHA" (Thermo Fisher Scientific, USA).

2.5 Computational chemical approaches

2.5.1 Quantum chemical calculations

To examine the correlation between the molecular structure and the reactivity of the Aripiprazole compound, theoretical calculations were carried out using DMol3 module established in Materials Studio version 7.0 and Gaussian 0.9 software.

2.5.2 Monte Carlo (MC) Simulation

MC simulations were carried out in a simulation box with periodic boundary conditions using the Materials Studio program version 7.0 (Accelrys Inc., San Diego, CA, USA). The pure CS crystal was used, and it was cleaved along with the most stable (lower energy) plane (1 1 0), resulting in a 30 vacuum slab. "The plane CS surface of (1 1 0) was relaxed by lowering its energy, and then the surface of CS (1 1 0) was extended to a supercell (10/10). The simulation analysis has been carried out in a test box containing the simulated corrosive species and inhibitor molecule, with the high-quality force field known as COMPASS being assigned to combine organic parameters and inorganic substances" [16].

3. RESULTS AND DISCUSSION

3.1. Weight loss (WL) method

The WL of CS in acidic solution at 25 °C in the absence and presence of a different concentration of Aripiprazole drug after various immersion periods (30-180) is shown in Figure 1. The WL was found to decreases as the drug concentration increases due to the formation layer on the CS surface. The adsorbed molecule isolates the metal from acidic solution and inhibits the corrosion sites [17] .
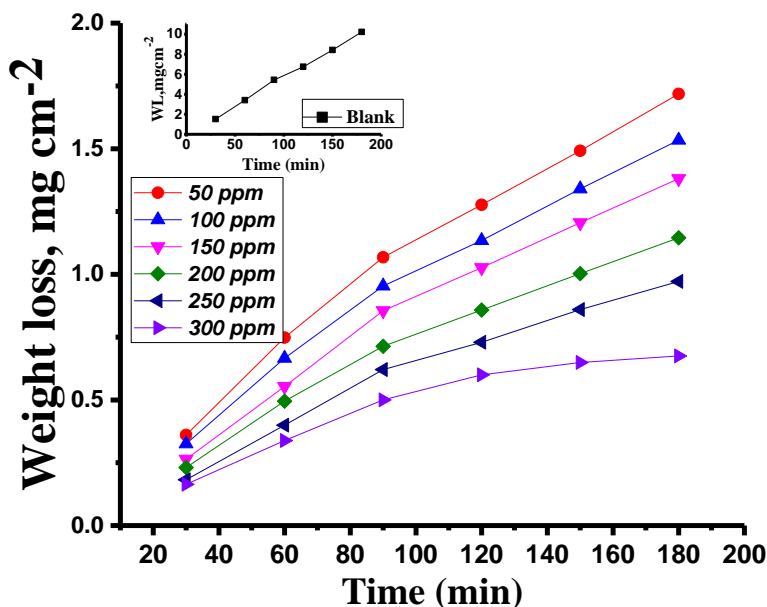
Figure 1. WL vs. time at 25°C for CS corrosion in 1 M HCl in the presence and absence of different concentrations of Aripiprazole drug

3.1.1. Influence of temperature

CR, θ, and % IE for CS in HCl (1 M) solution in the absence and presence of different concentrations of Aripiprazole at various temperatures were indicated in Table 2. The CR decreased

while θ and % IE raised with increased concentration of Aripiprazole and this improving decrease with increasing temperature. This shows the physical adsorption of the Aripiprazole drug on the CS.

Table 2. CR, θ, and % IE of CS in HCl (1 M) solution in the presence and absence of different concentrations of Aripiprazole concentration.

| Temp. (°C)	Conc.(ppm)	CR (mg cm^{-2} min^{-1})	Θ	% IE
25	Blank	0.086	----	----
	50	0.01	0.884	88.4
	100	0.0087	0.899	89.9
	150	0.0081	0.906	90.6
	200	0.0078	0.909	90.9
	250	0.0064	0.926	92.6
	300	0.0059	0.931	93.1
30	Blank	0.094	----	----
	50	0.0158	0.832	83.2
	100	0.016	0.830	83.0
	150	0.0136	0.855	85.5
	200	0.0131	0.861	86.1
	250	0.0098	0.896	89.6
	300	0.0085	0.910	91.0
35	Blank	0.115	----	----
	50	0.029	0.748	74.8
	100	0.0241	0.790	79.0
	150	0.0212	0.816	81.6
	200	0.0182	0.842	84.2
	250	0.0168	0.854	85.4
	300	0.0129	0.888	88.8
40	Blank	0.162	----	----
	50	0.042	0.741	74.1
	100	0.038	0.765	76.5
	150	0.0346	0.786	78.6
	200	0.031	0.809	80.9
	250	0.0283	0.825	82.5
	300	0.0242	0.851	85.1
45	Blank	0.184	----	-----
	50	0.063	0.658	65.8
	100	0.058	0.685	68.5
	150	0.0461	0.749	74.9
	200	0.0411	0.777	77.7
	250	0.0361	0.804	80.4
	300	0.0301	0.836	83.6

The activation energy (E_a^*) was estimated from the Arrhenius equation as follow [18]:

$$\text{Log CR} = \log A - (E_a^*/2.303R)\ 1/T \qquad (5)$$

Where A refers to the Arrhenius pre-exponential factor. Figure 2 shows plotted of log CR and 1/T with different concentrations of Aripiprazole. E_a^* values can be calculated. ΔH^* and ΔS^* can be determined using the following transition state equation [19]:

$$CR = RT/ Nh\ \exp (\Delta S^*/ R)\ \exp (-\Delta H^*/ RT) \qquad (6)$$

Where h refers the Planck's constant. Figure 3 shows log (CR/T) vs 1/T diagrams for different concentrations of Aripiprazole. ΔH^* and ΔS^* were determined from the slopes and intercepts of the straight lines. Thermodynamic activation parameters were displayed in Table 3. This illustrated the values of E_a^* for solutions containing Aripiprazole where they're higher than the blank solution. The increase in the E_a^* indicates Aripiprazole particles are physisorbed on the CS surface. The positive signs of ΔH^* values indicate an endothermic activation process. The increase in values of ΔH^* in inhibited solutions compared with the uninhibited ones designates that the energy barrier in the dissolution reaction improved. The variance between E_a^* and ΔH^* values is exactly 2.6 kJ mol^{-1}, which is almost near to the RT worth (2.63 kJ mol^{-1}) [20]. The negative signs of ΔS^* demonstrate that the disorder decrease via the path from the reactant to the activated complex [21].
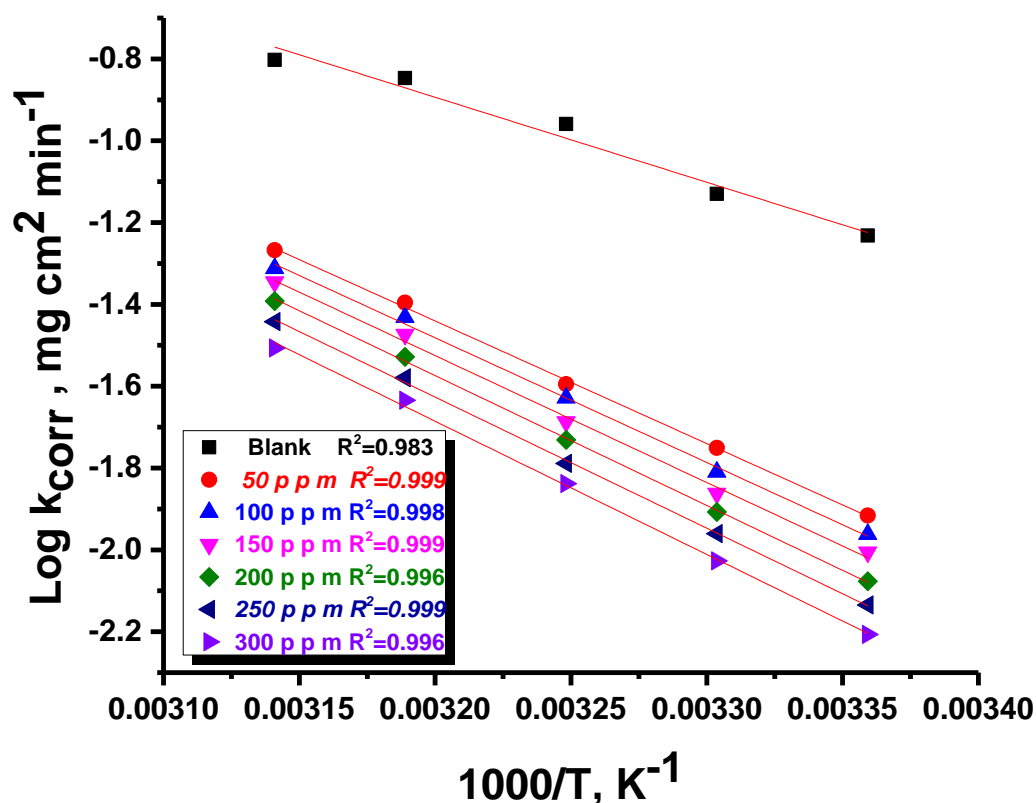
Figure 2. log CR vs. 1/T curves in the absence and presence of different concentrations of Aripiprazole for corrosion of CS in 1 M HCl
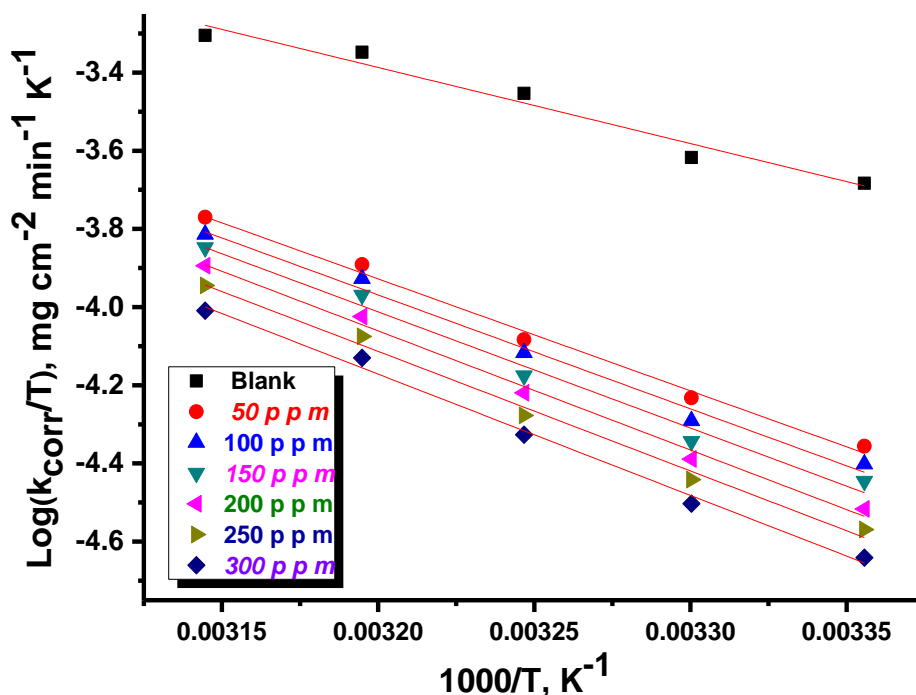
Figure 3. log (CR/T) vs. 1/T diagram without and with of different concentrations of Aripiprazole for corrosion of CS in 1 M HCl

Table 3. Thermodynamic activation parameters in the absence and presence of different concentrations of Aripiprazole for CS corrosion in 1 M HCl

| Conc, ppm	E_a^*, kJ /mol	ΔH^*, kJ /mol	$-\Delta S^*$, J /mol.K
Blank	39.8	37.2	143
50	57.4	54.8	97
100	58.3	55.7	94
150	59.4	56.8	92
200	60.7	58.3	88
250	61.3	58.6	88
300	62.3	59.4	87

3.1.2. Adsorption isotherm

Aripiprazole drug is adsorbed on the CS surface due to the communicating energy between the CS surface and the drug is more than between H_2O and metal [22]. The Langmuir isotherms model adsorption match in an excellent way from the data (Figure 4). The Langmuir isotherm can be represented by the next Eq. [23]
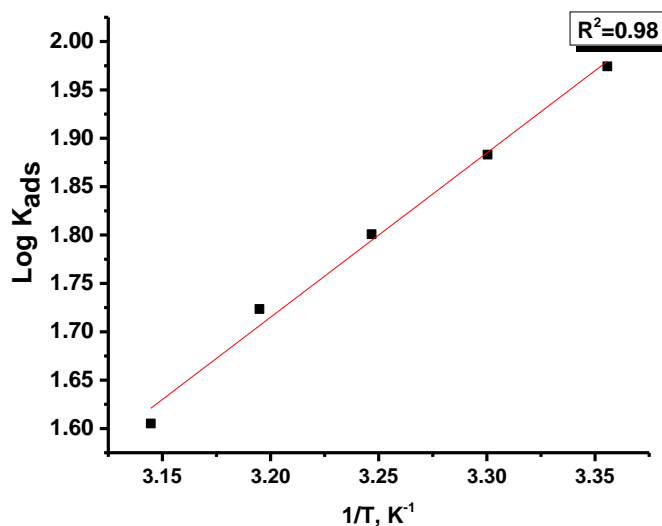
$$C/\theta = 1/K_{ads} + C \qquad (7)$$

with K_{ads}= adsorption constant and C= concentration of Aripiprazole. ΔG^o_{ads} can be obtained by applying the following Eq.

$$\log K_{ads} = 1/55.5 \exp (\Delta G^o_{ads} /2.303RT) \qquad (8)$$

With 55.5 as water concentration (mole L^{-1}) at the CS/solution interface.
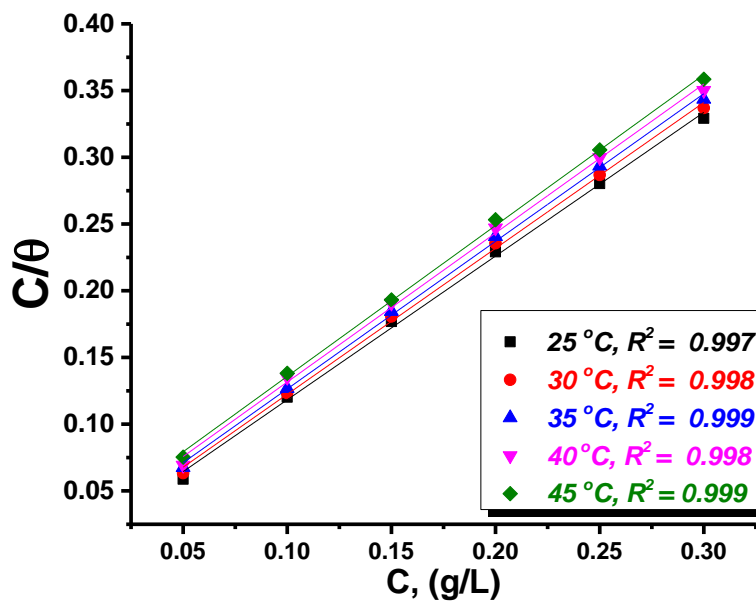
Figure 4. Langmuir model of Aripiprazole drug on CS surface at different temperatures.

Figure 5. Log K_{ads} vs. 1/T curve for adsorption of Aripiprazole drug on the CS surface.

The enthalpy of adsorption (ΔH^o_{ads}) was obtained by applying Vant't Hoff Eq. as following [24]:

$$\log K_{ads} = -\Delta H^o_{ads}/2.303RT + \text{constant} \qquad (9)$$

Figure 5 shows plotted between log K_{ads} and 1/T. From the slope of the line, ΔH^o_{ads} value can be calculated. The entropy of adsorption (ΔS^o_{ads}) can be obtained by applying the following Eq.

$$\Delta S^o_{ads} = (\Delta H^o_{ads} - \Delta G^o_{ads})/T \qquad (10)$$

The obtained adsorption parameters were listed in Table 4. The negative values of ΔG^o_{ads} indicated that the adsorption procedure of the Aripiprazole on the CS surface is spontaneous. The obtained data of ΔG^o_{ads}, are around 20 kJ mol^{-1} indicates physisorption between the Aripiprazole and CS surface. ΔH^o_{ads} is negative indicates that the adsorption procedure is exothermic. The negative values of ΔS^o_{ads} indicate that there was a decrease in entropy accompanying the adsorption process.

Table 4. Adsorption parameters for Aripiprazole on CS at different temperatures.

T K	K_{ads} M^{-1}	$-\Delta G^o_{ads}$ kJ mol^{-1}	$-\Delta H^{\circ}_{ads}$ kJ mol^{-1}	$-\Delta S^{\circ}_{ads}$ J mol^{-1}K^{-1}
298	94	21.2		38
303	76	21.0		37.9
308	63	20.9	32.5	39.7
313	52	20.7		37.5
318	40	20.3		37.2

3.2 Potentiodynamic polarization (PP) method

Figure 6 shows the PP bends for the CS metal in 1M HCl solution in the absence and presence different concentrations of the tested Aripiprazole drug at 25 °C.
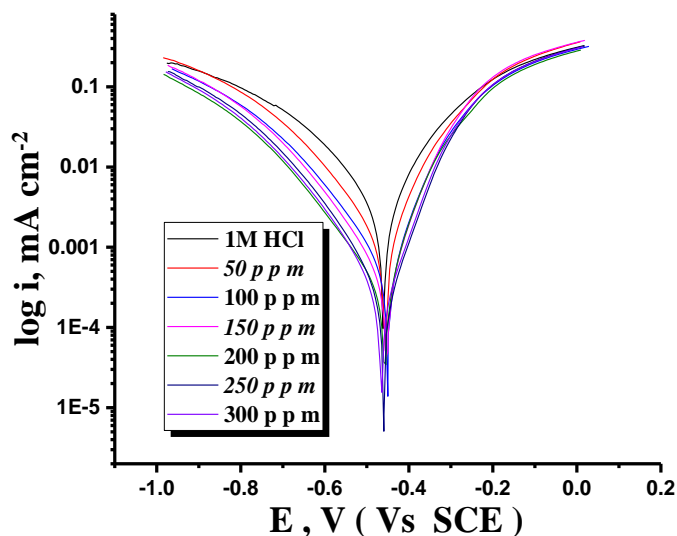
Figure 6. PP curves for CS metal in the 1M HCl solution at different concentrations of Aripiprazole drug at 25°C

Polarization parameters such as the (i_{corr}), (E_{corr}) for blank and inhibited specimen at various concentrations, (β_c & βa), and (%IE)) for the Aripiprazole drug are shown in Table 5. The %IE was calculated using the previous relation. It noticed that with decreasing the (i_{corr}), inhibition efficiency values increase as inhibitor concentration increases as in Table 5. The inhibitor can be anodic or cathodic if E_{corr} is greater than -85mV/SCE compared to the potential for the corrosion of uninhibited blank, whereas the inhibitor can be considered a mixed form if E_{corr} is less than -85mV/SCE, [25]. In our research, the shift was less than -11 mV/SCE, signifying that the Aripiprazole drug is a mixed type [26][27].

Table 5. PP parameters for CS metal in 1M HCl without and with different concentrations of the tested Aripiprazole drug at 25°C

Conc. ppm	i_{corr} $\mu A/cm^{-2}$	$-E_{corr.}$ mV(SCE)	β_a mV dec^{-1}	β_c mV dec^{-1}	CR mpy	Θ	% IE
Blank	2360	461	107	147	1080	--	--
50	732	457	85	131	453	0.690	69.0
100	517	450	83	141	291	0.781	78.1
150	318	453	80	134	191	0.865	86.5
200	201	457	75	140	134	0.915	91.5
250	169	459	88	133	130	0.928	92.8
300	122	460	81	135	107	0.948	94.8

3.3. Electrochemical impedance spectroscopy (EIS) tests:

One of the exact tests used to check the corrosion process is EIS [28]. Figure (7) shown the equivalent circuit utilized to fit the EIS measurements. The resulting Nyquist graphs were seen in Figure 8. It is noticed that the semicircle diameter of the Nyquist plot increased progressively when the Aripiprazole concentration was increased from 50 to 300 ppm. Table 6 contains different parameters, including solution resistance (R_s), the phase shift (n), double layer capacitance (C_{dl}), charge transferred resistance (R_{ct}), (Θ), and (%IE) obtained from the EIS test. It is noticed that the (R_{ct}) values increase while the (C_{dl}) values gradually decrease as the concentration of the Aripiprazole drug increases; this can be demonstrated by the incremental substitution of water molecules by the drug molecule that adsorbed on the metal surface, which results in the reduction of the metal dissolution reaction. The C_{dl} is mathematically expressed as in next balance:

$$C_{dl} = Y_0 (\omega_{max})^{n-1} \qquad (11)$$

Where Y_0 is the magnitude of the CPE and (n) represents the deviation from the ideal behavior. During investigations, we notice that the n values are in the range ($0 \leq n \leq 1$) and this occurs for many reasons, containing surface heterogeneity, electrode roughness, and dielectric constant. The result gotten from the n value in one molar HCl alone is higher than the results achieved in the presence of various concentrations of the Aripiprazole drug. The n values lie in range (0.887 - 0.761), deviation from unity

can be illustrated based on heterogeneity and roughness occurred on the CS surface [29]. High resistance has been obtained as a result of Aripiprazole adsorption at the CS solution/interface.
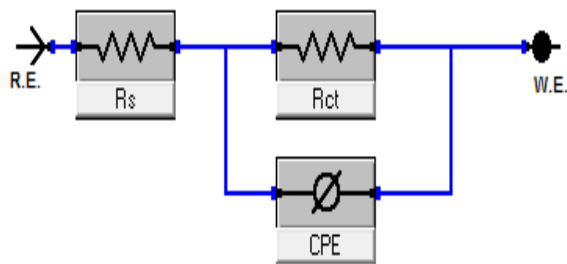

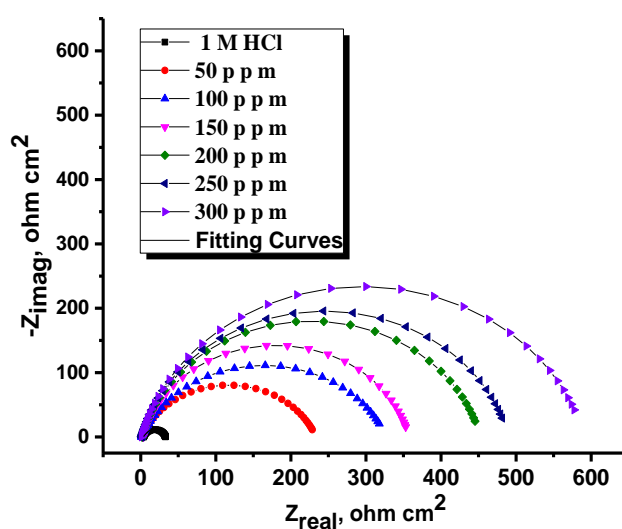**Figure 7.** A simple circuit was utilized to fit the EIS data.

Figure 8. The Nyquist diagram for CS dissolution in presence and absence of different concentration of Aripiprazole drug**.**
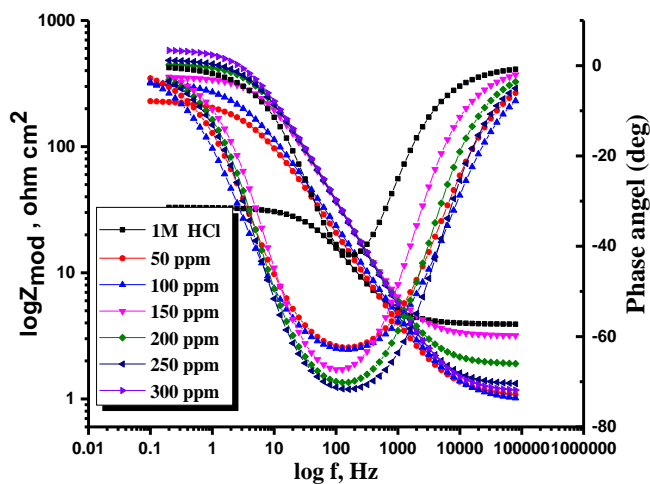

Figure 9. The Bode diagram for corrosion of CS in presence and absence of different concentration of Aripiprazole drug**.**

Table 6. EIS parameters for the dissolution of CS in 1.0 M HCl in the presence and absence of Aripiprazole drug

| Conc., ppm	Y_o, $(\mu\,\Omega^{-1}\,s^n\,cm^{-2})\,x10^{-6}$	n	R_{ct}, $\Omega\,cm^2$	C_{dl}, $\mu F\,cm^{-2}$	Θ	% I.E
1 M HCl	332	0.887	29	143	---	---
50 ppm	242	0.771	233	103	0.876	87.6
100 ppm	210	0.761	327	91	0.911	91.1
150 ppm	106	0.862	354	63	0.918	91.8
200 ppm	101	0.858	450	61	0.936	93.6
250 ppm	98	0859	488	59	0.941	94.1
300 ppm	93	0.841	589	53	0.951	95.1

3.4. Atomic force microscopy (AFM) analysis

AFM produces ideal microscopic images of CS surface, allowing the roughness of the examined metal to be assessed. Figure 10 shows the 3D AFM morphologies for CS in 1M HCl in the presence and absence of the Aripiprazole drug. The roughness of the CS surface in 1M HCl is higher (993.8 nm), indicating that the CS blank sample has been heavily corroded by corrosive attacks. The obtained roughness of inhibited CS (shown in Figure10) was reduced to low values (94 nm) due to the effectiveness of the adsorbed layer of inhibitor on the surface, preventing dissolution of CS [30].
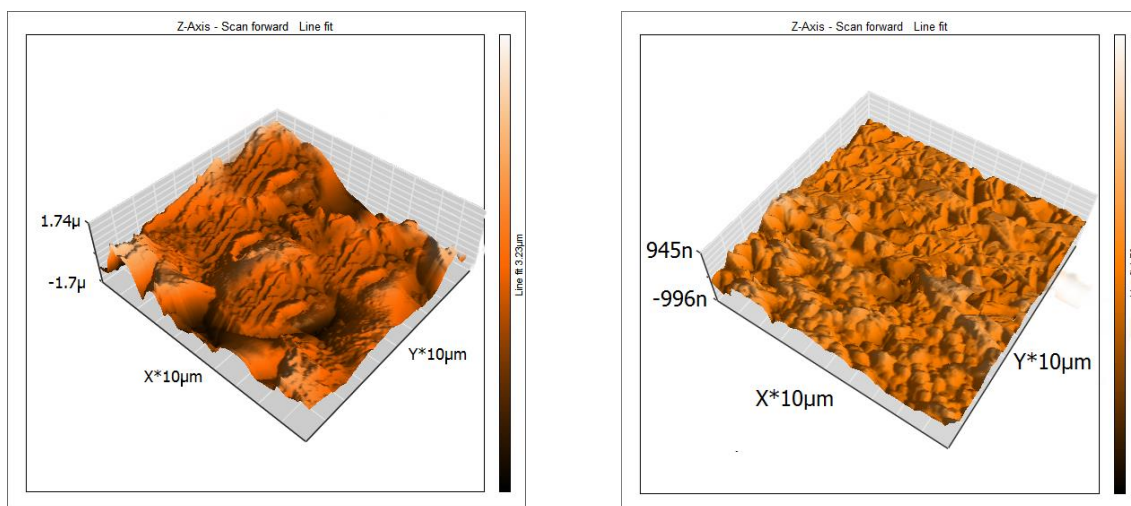
Figure 10. AFM 3D images of: A) CS in 1M HCl only, B) CS in 1M HCl + 300ppm of the Aripiprazole drug.

### 3.5. Fourier transform infrared spectroscopy (FT-IR) analysis

The FT-IR spectrophotometer is an effective instrument employed for identifying the functional groups that are present in the Aripiprazole drug and the kind of interaction that occurs between the function group and metal surface[31]. Figure 11 displays broad peaks of Aripiprazole drug and Aripiprazole drug with CS. It is clear that there is some peaks displacement between the spectra of the Aripiprazole drug and the adsorbed drug from CS surface after corrosion, also a few peaks are disappearing or be with less eminent[32]. This indicates the interaction of the Aripiprazole drug with CS through the functional groups present in the Aripiprazole drug molecule, resulting in the protection from corrosion occurred.
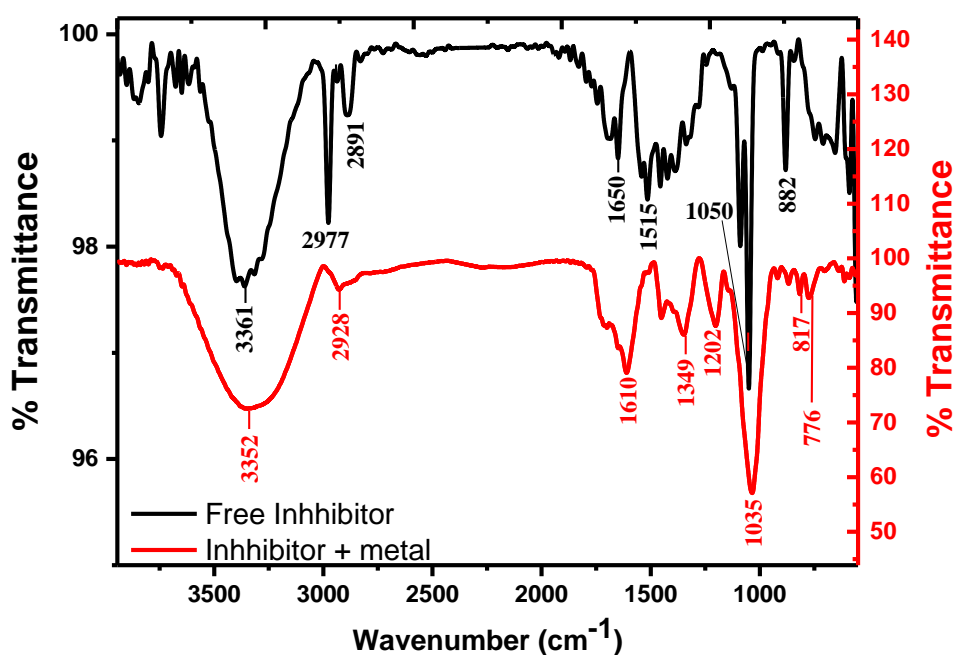
Figure 11. FT-IR spectra for Aripiprazole drug and for Aripiprazole drug + CS metal

3.6. X-ray photoelectron spectroscopy (XPS) examination

The XPS analysis of the Aripiprazole drug focused on definite atoms such as (C, O, N, Cl, and Fe), with the results displayed in Figure12 for CS after immersion in 1M HCl at 25°C with 300 ppm of Aripiprazole drug. Table 7 indicates the peaks binding energies (BE, eV) and the corresponding assignment [33]. The results of XPS analysis confirm the adsorption of Aripiprazole drug on CS surface in 1 M HCl.
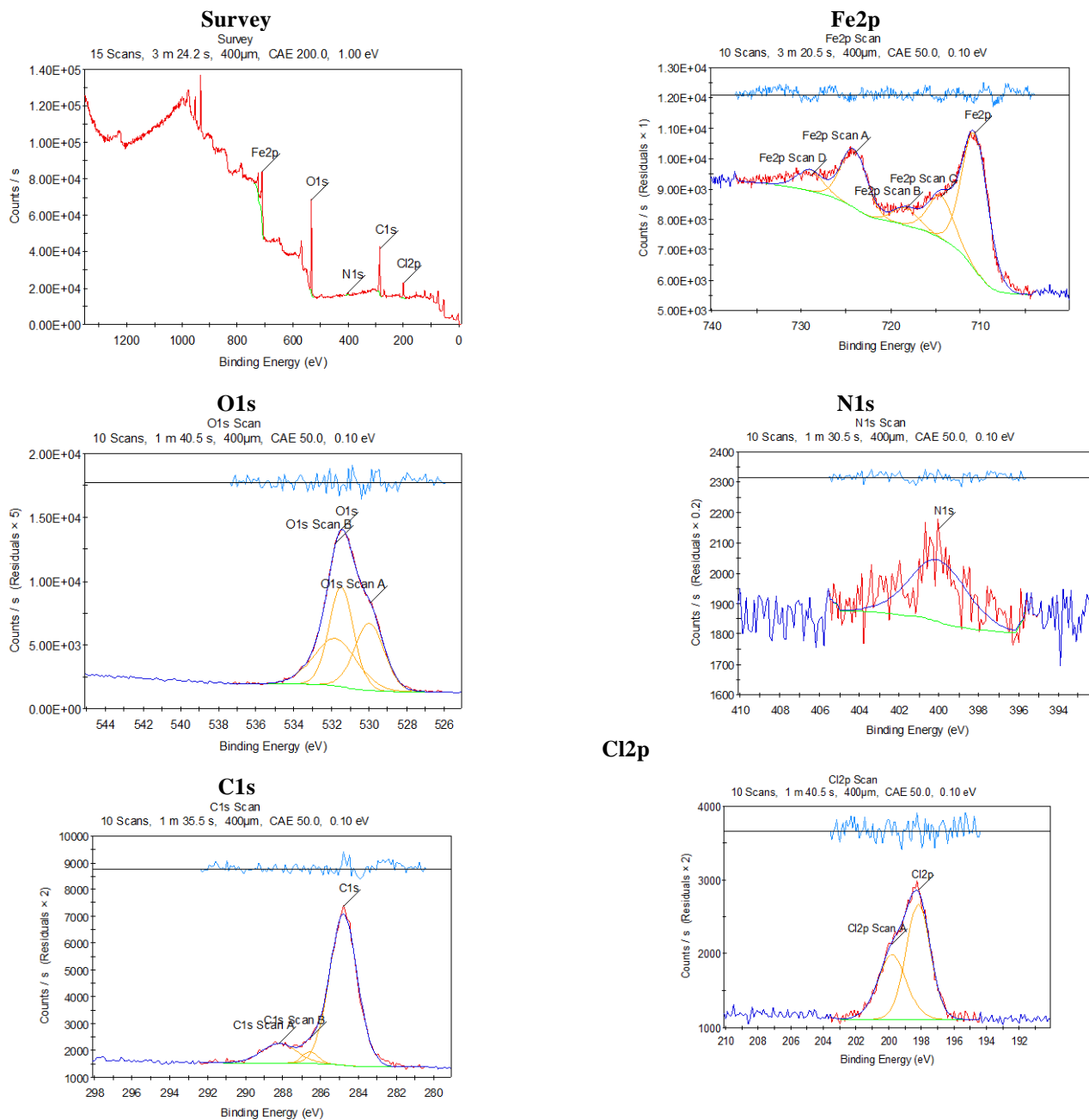
Figure 12. XPS diagrams of a survey, C1s scan, O1s scan, N1s scan, Cl2p scan, Fe2p scan of CS after immersion in 1 M HCl+300ppm of Aripiprazole drug inhibitor for 24 h.

Table 7. Binding energies (eV) of the core elements for inhibited CS surface as results from XPS analysis

Core element	BE, eV	Assignments
C1s	285.17	C-C,
	286.91	-C=O,C-H
	288.34	C-$^+$O, C-S,C=N, C-$^+$N,C=O
O1s	537.38	Metal oxide, Hydroxide, FeO and Fe_2O_3

	531.87	
	530.03	
N1s	400.03	N-Fe
Fe2p	710.59	Metallic iron Fe2p$_{1/2}$ of Fe^{3+} Fe$_2$O$_3$/ Fe$_3$O$_4$/ FeOOH FeCl$_3$
	724.07	
	718.34	
	714.41	
	728.99	
Cl2p	198.8	Cl 2p3/2

3.7. Theoretical calculations

3.7.1 Quantum Chemical Parameters

The quantum chemistry, according to the DMol3 module established in Materials Studio version 7.0 and the Gaussian 09 software was utilized for all calculations in the current research [34]. The optimized structures have been used as input structures for further optimization using the following high-level methods: HF/6-31++G(d,p), and DFT/B3LYP/6- 31++G(d,p) [35][36]. The analysis of the density distributions optimized geometry, highest occupied molecular orbital (HOMO), and lowest unoccupied molecular orbital (LUMO) structures of the inhibitors are shown in Figure 13. HOMO and LUMO can determine the donation - acceptance capacity and the molecular reactivity of the Aripiprazole drug. E_{HOMO} denotes the ability of the molecule to donate electron, whereas E_{LUMO} describes the ability of the molecule to accept electron. The dipolar moment (μ) is a measure of the polarity with the covalent bond [25].

The energy band gap ΔE_g ($\Delta E = E_{HOMO} - E_{LUMO}$) that the lower energy gap value is considered to be high reactivity molecule and have a good corrosion inhibition efficiency onto the metal surface [37]. The quantum parameters association with corrosion inhibition were calculated including E_{HOMO} and E_{LUMO} values, frontier orbital energy gap, molecular dipole moment (μ), electron affinity (E_A), ionization potential (I_p), electronegativity (χ), global hardness (η) that are used to calculate the electrons transfer from the inhibitor molecule to the metallic atom ΔN, softness (σ), electrophilicity index (ω) and back-donation (ΔE back-donation), were calculated as Koopmans's theorem [38] from the following equations:

$$I_p = -E_{HOMO}, \quad E_A = -E_{LUMO} \tag{12}$$

$$\mu = -\chi = -\frac{I_p + E_A}{2} \tag{13}$$

$$\chi = \frac{I_p + E_A}{2} \tag{14}$$

$$\eta = \frac{I_P - E_A}{2} \tag{15}$$

$$\sigma = \frac{1}{\eta} \tag{16}$$

$$\omega = \frac{\mu^2}{2\eta} \tag{17}$$

$$\Delta E_{back\ donation} = -\frac{\eta}{4} \tag{18}$$

$$\Delta N = \frac{(\chi Fe - \chi inh)}{2(\eta Fe + \eta inh)} \tag{19}$$

"Where χ_{Fe}, χ_{inh} η_{Fe}, and η_{inh} are the absolute electronegativity of iron, inhibitor molecule, the absolute hardness of iron, and the inhibitor molecule, respectively [39]. a theoretical value of $\chi Fe = +7.0$ eV [40] and $\eta Fe = 0$ $(eV)-1$ by assuming that for a metallic bulk I = A, because they are softer than the neutral metallic atoms [41]. The ΔE back donation implies that when $\eta > 0$ and $\Delta E_{\text{back donation}} < 0$ the charge-transfer to a molecule", followed by aback donation from the molecule, is energetically favored.

|	DMol3	HF	DFT
Molecular orbital			
HOMO			
LUMO			
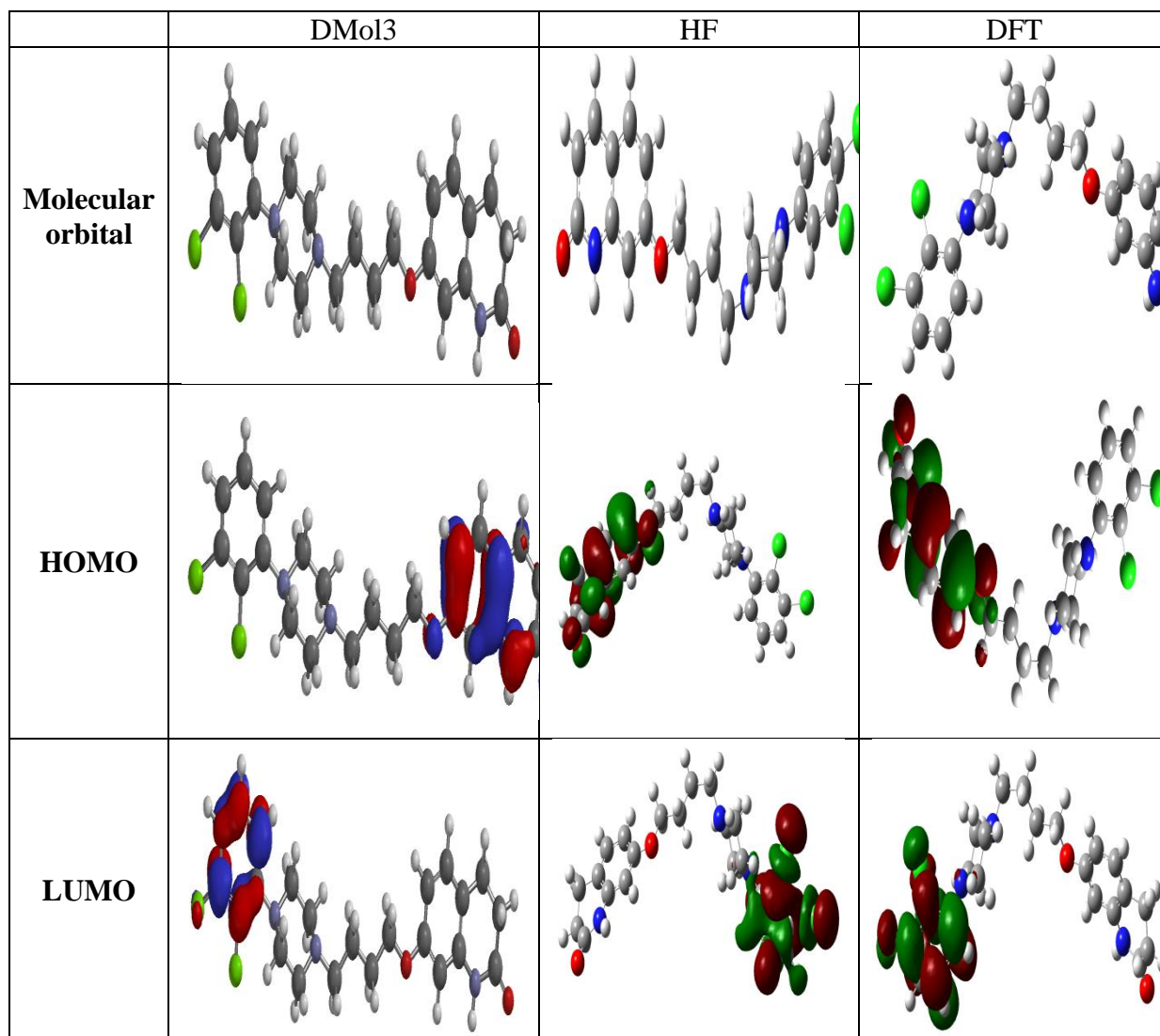
Figure 13. The frontier molecular provides the electron density maps of HOMO, and LUMO for the Aripiprazole.

Table 7. Quantum calculation parameters for Aripiprazole molecule obtained from DMol3, HF, and DFT.

Parameters (Variable)	DMol3	HF	DFT
E_{HOMO} (ev)	-8.86	-0.317	-1.048
E_{LUMO} (ev)	-0.18	0.109	0.7809
ΔE, (eV) (E_L-E_H)	8.68	0.426	1.8289
μ (debye) (Dipole moment)	3.88	2.11	5.36
A (eV) (electron affinity)	0.18	-0.109	-0.7809
I (eV) (ionization potential)	8.86	0.317	1.048
χ (eV) (electronegativity)	4.52	0.104	0.134
η (eV) (global hardness)	4.34	0.213	0.915
ΔN	0.286	16.19	3.75
σ (eV^{-1}) (softness)	0.23	4.69	1.09
ω (eV) (electrophilicity index)	1.73	10.45	13.14
Back-donation (ΔE)	-1.085	-0.053	-0.229

3.7.2 Monte Carlo (MC) Simulation

MC modeling is an excellent method for determining the most stable adsorption conformations of a pharmaceutical molecule in 1M HCl. Figure 14 illustrates the simulation findings for the investigated pharmaceutical, which are described in Table 8. Figure 14 depicts the adsorbed molecule's most favorable confirmation on the Fe metal surface (110). Furthermore, the molecules stated are adsorbed on the metal surface from the motive, which is rich in inhibitory molecule electrons. The interactions between the occupied orbitals of the examined Aripiprazole drug and the vacant orbitals of Fe (110), which are reflected by energy adsorption values (E_{ads}), of the rigid energy (E_{rigid}), of the deformation energy (E_{def}), and energy ratio values (dE_{ads}/dN_i) of the inhibitors, which is equivalent to the energy of substrate-adsorbate configurations where one of the adsorbate components has been removed are collected in Table 8. Adsorption energy values that are more negative indicate a highly stable and strong connection between adsorbed molecules and metal. When two materials are mixed during the adsorption process, an electron, ion, or molecule (adsorbent) is attached to the solid surface, adsorption energy is defined as declining energy [42]. As shown in Table 8, the greater adsorption energy of Aripiprazole molecules on the hardened Fe surface predicts heavy adsorption of Aripiprazole molecules, forming a stable adsorbed layer that protects the iron from decomposition.
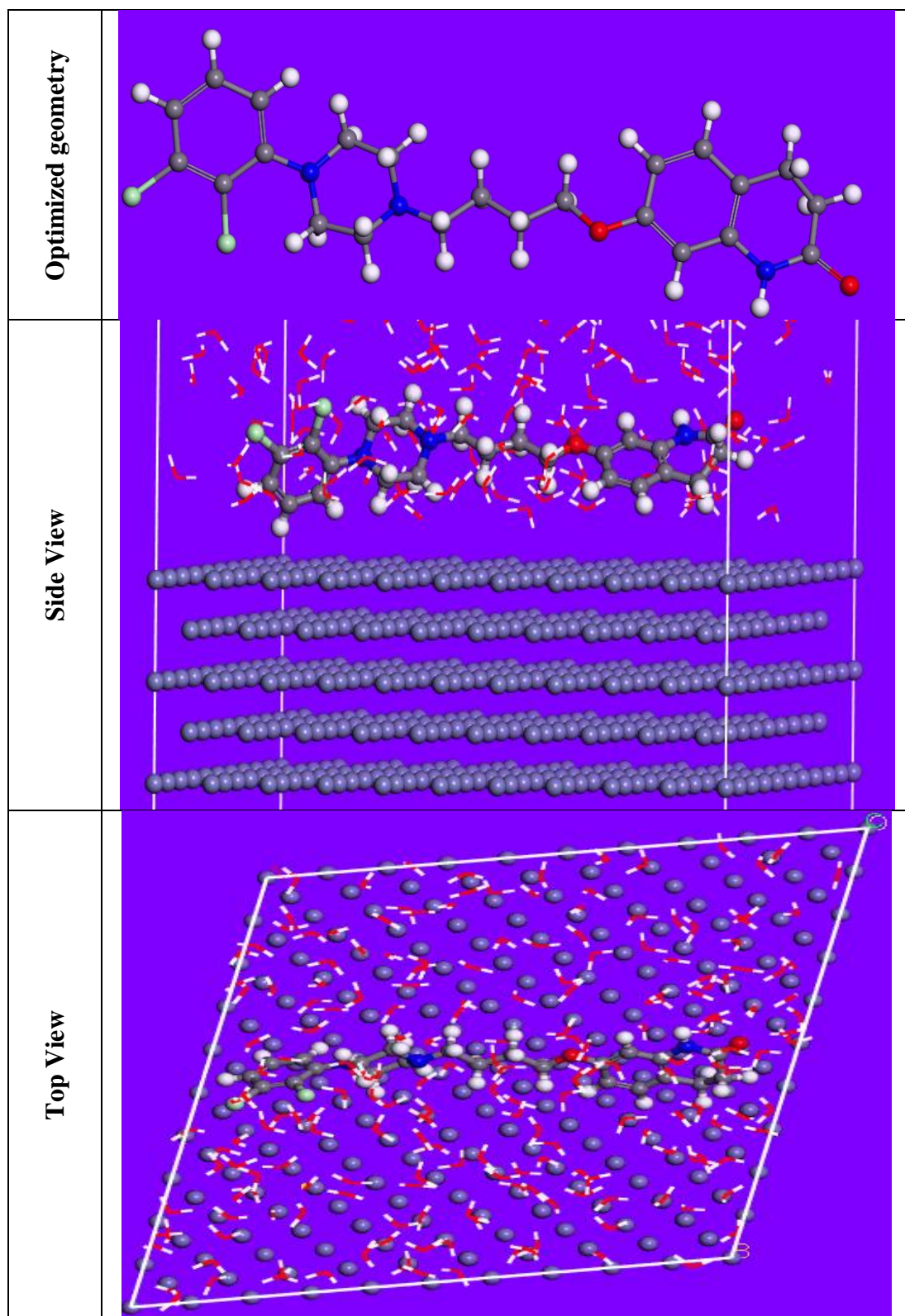
Figure 14. The most suitable configuration for adsorption of the drug molecule on Fe (1 1 0) substrate obtained by adsorption locator module.

Table 8. Data and descriptors calculated by the Monte Carlo simulation for adsorption of drug molecule on Fe (1 1 0).

Structures	Total energy	Adsorption energy	Rigid adsorption energy	Deformation Energy	Compound dE_{ad}/dN_i	H_2O dE_{ad}/dN_i
Fe (1 0 0)/ MA-1232 /H$_2$O	-3211.16	-4108.929	-4039.791	-69.138	-263.097	-12.522

3.8. Corrosion Inhibition Mechanism

The adsorption of investigated Aripiprazole drug at the CS surface can happen among its active sites of N and O atoms in addition to a π electron interaction of the benzene ring. The pure CS is negatively charged at E_{ocp} due to adsorbed Cl$^-$ ion. Aripiprazole drug can be protonated in an acid medium and become a cationic molecule. So, the cationic form of the protonated Aripiprazole drug molecules can adsorb on the negative charge metal surface by electrostatic attraction forces forming physical adsorption Figure 14. Aripiprazole drug is an efficient inhibitor because it has 3 N and 2 O atoms active sites, 2 benzene rings, and has a high molecular size that covers more surface area.
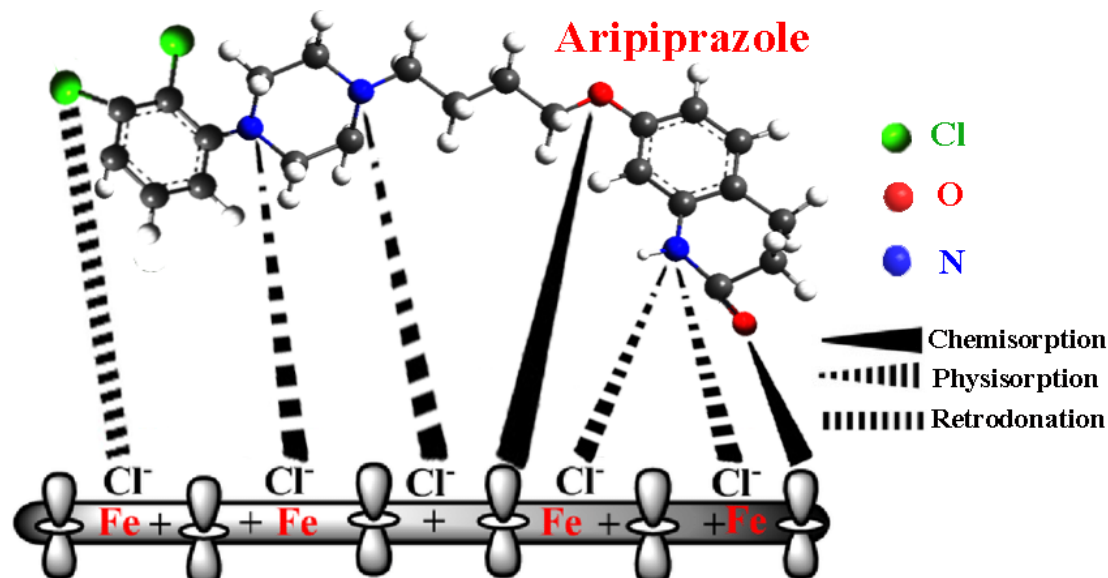
Figure 14. Corrosion inhibition mechanism of CS by expired Aripiprazole green inhibitor in 1M hydrochloric acid solution

Pharmaceutical compound inhibitors have pulled attention to the cost-effective way of preventing acid corrosion. A great number of drug compound used in acidic solution for protection against corrosion for CS [43][30][44][45][46][47]. Table 8 shows the percent IE of the Aripiprazole drug and some of the previously mentioned products. The %IE of current Aripiprazole drugs is higher than obtaining from previously reported drugs, as seen in Table 8.

Table 8. % IE obtained for certain drugs tested by other authors was compared to obtain in this study.

Inhibitor (drug)	Sample	Medium	IE %	References
Ciprofoxacin (50 ppm)	Mild steel	HCl	20.8	[37]
Penicillin V (15×10^{-4}M)	Mild steel	H_2SO_4	63.3	[38]
Cefalexin (11×10^{-4}M)	Mild steel	HCl	67.5	[39]
Tenoxicam (4×10^{-4}M)	Carbon steel	HCl	81	[40]
dichlorphenamide (50 ppm)	Carbon steel	HCl	81.5	[41]
Niclosamide (50 ppm)	Carbon steel	HCl	86.6	[41]
Mesalazine (800 ppm)	Carbon steel	H_2SO_4	89.5	[42]
Aripiprazole	Carbon steel	**HCl**	**95.1**	**This study**

4. CONCLUSIONS

The investigated Aripiprazole drug in 1.0 M HCl solution can use as an effective corrosion inhibitor for CS. Aripiprazole drug has an inhibition capacity of 95.1 percent. The percentage of %IE increases by raising Aripiprazole concentration and lower temperature. This suggests that the Aripiprazole drug being studied are physically adsorbed. The adsorption of the Aripiprazole drug was obeying isothermal Langmuir adsorption. Tafel constant values (βa and βc) confirm the drug is a mixed type. The electronic molecular parameters (HOMO and LUMO) emphasize the mechanisms of green inhibitor aripiprazole on the CS surfaces. This study illustrates that the Aripiprazole drug has been confirmed to be a significant, environmentally friendly one and low-cost inhibitor.

References

1. A. Khadiri, R. Saddik, K. Bekkouche, A. Aouniti, B. Hammouti, N. Benchat, M. Bouachrine, R. Solmaz, Gravimetric, *J. Taiwan Inst. Chem. Eng*., 58 (2016) 552.
2. A. Lalitha, S. Ramesh, S. Rajeswari, *Electrochim Acta*., 51 (2005) 47.
3. A.S. Fouda, M.A.A.A. El-Ghaffar, M.H. Sherif, A.T. El-Habab, A. El-Hossiany, *Prot. Met. Phys. Chem. Surfaces*, 56 (2020) 189.
4. A.S. Fouda, M. Eissa, A. El-Hossiany, *Int. J. Electrochem. Sci*., 13 (2018) 11096.
5. A.Y. Musa, A.A.H. Kadhum, A.B. Mohamad, M.S. Takriff, A.R. Daud, S.K. Kamarudin, *Corros. Sci.*, 52 (2010) 526.
6. N.O. Eddy, E. E. Ebenso, *Int. J. Electrochem. Sci*., 5 (2010) 731.
7. H. Vashisht, I. Bahadur, S. Kumar, G. Singh, D. Ramjugernath, E.E. Ebenso, *Int. J. Electrochem. Sci.,* 9 (2014) 5204.
8. M. Abdallah, *Port. Electrochim. Acta*., 22 (2004) 161.
9. A. Khadiri, R. Saddik, K. Bekkouche, A. Aouniti, B. Hammouti, N. Benchat, M. Bouachrine, R. Solmaz, Gravimetric, *J. Taiwan Inst. Chem. Eng*., 58 (2016) 552.
10. M. M. Solomon, S. A. Umoren, I. I. Udosoro, A. P. Udoh, *Corros. Sci*., 52 (2010) 1317.
11. F. G. Liu, M. Du, J. Zhang, M. Qiu, *Corros. Sci*., 51 (2009) 102.
12. S. Leucht, A. Crippa, S. Siafis, M. X. Patel, N. Orsini, J. M. Davis, *Am. J. Psychiatry*, 177 (2020)

    342.
13. G. Ostuzzi, I. Bighelli, R. So, T.A. Furukawa, C. Barbui, *Schizophr. Res*., 183 (2017) 10.
14. A.S. Fouda, E. Abdel-Latif, H.M. Helal, A. El-Hossiany, *Russ. J. Electrochem*., 57 (2021) 159.
15. R. Kalaivani, B. Narayanaswamy, J. A. Selvi, A.J. Amalraj, J. Jeyasundari, S. Rajendran, *Port. Electrochim. Acta.,* 27 (2009) 177.
16. K. R. Ansari, M. A. Quraishi, *J. Taiwan Inst. Chem. Eng*., 54 (2015) 145.
17. G. Gece, Corros. Sci., 53 (2011) 3873.
18. A.S. Fouda, H. Ibrahim, S. Rashwaan, A. El-Hossiany, R.M. Ahmed, *Int. J. Electrochem. Sci*., 13 (2018) 6327.
19. H. M. Abd El-Lateef, K. A. Soliman, A. H. Tantawy, *J. Mol. Liq*., 232 (2017) 478.
20. S. K. Shukla, M. A. Quraishi, *Mater. Chem. Phys*., 120 (2010) 142.
21. O. A. Hazazi, M. Abdallah, *Int. J. Electrochem. Sci*., 8 (2013) 8138.
22. O. A. Hazazi, M. Abdallah, *Int. J. Electrochem. Sci*., 8 (2013) 8138.
23. X. Li, S. Deng, H. Fu, *Corros. Sci*., 51 (2009) 1344.
24. M. M. Motawea, A. El-Hossiany, A. S. Fouda, *Int. J. Electrochem. Sci*., 14 (2019) 1372.
25. K. D. C. R. Jahromi, *Int. J. Curr. Res*., 9(1) (2017) 44630.
26. A. S. Fouda, R. E. Ahmed, A. El-Hossiany, *Prot. Met. Phys. Chem. Surfaces*, 57 (2021) 398.
27. A. S. Fouda, S. Rashwan, A. El-Hossiany, F. E. El-Morsy, *J. Chem. Bio. Phy. Sci*., 9 (2019) 001.
28. I. Lukovits, K. Palfi, E. Kalman, Corrosion, 53 (1997) 915.
29. A. S. Fouda, E. El-Gharkawy, H. Ramadan, A. El-Hossiany, *Biointerface Res. Appl. Chem*., 11(2) (2021) 9786.
30. N. O. Eddy, S. A. Odoemelam, *Adv. Nat. Appl. Sci*., 2 (2008) 225.
31. A. K. Singh, M. A. Quraishi, *J. Appl. Electrochem*., 41 (2011) 7.
32. A. S. Fouda, M. A. Azeem, S. Mohamed, A. El-Desouky, *Int. J. Electrochem. Sci*., 14 (2019) 3932.
33. O. A. Elgyar, A. M. Ouf, A. El-Hossiany, A.S. Fouda, *Biointerface Res. Appl. Chem*., 11(6) (2021) 14344.
34. J. Liu, W. Yu, J. Zhang, S. Hu, L. You, G. Qiao, *Appl. Surf. Sci*., 256(14) (2010) 4729.
35. M. A. Khaled, M. A. Ismail, A. A. El-Hossiany, A. S. Fouda*, RSC Adv*., 11 (2021) 25314.
36. J. H. Shuangkou, C. M. Xu, Q. Tang, Z. Yang, X. Tan, B. He, *Int. J. Electrochem. Sci.,* 16 (2021) 1.
37. S. K. S. H. Kumar, *J. Mater. Environ. Sci*., 3(5) (2012) 925.
38. T. Koopmans, *Physica*., 1 (1934) 104.
39. V. S. Sastri, J. R. Perumareddi, *Corros. Sci*., 53 (1997) 617.
40. M.S. Morad, *Corros. Sci.,* 50(2) (2008) 436.
41. M. J. Dewar, W. Thiel, *J. Am. Chem. Soc*., 99 (15) (1977) 4899.
42. A. Kosari, M.H. Moayed, A. Davoodi, R. Parvizi, M. Momeni, H. Eshghi, H. Moradi, *Corros. Sci*., 78 (2014) 138.
43. S. Acharya, S. N. Upadhyay, *Trans. Indian Inst. Met*., 57 (2004) 297.
44. A. K. Singh, M. A. Quraishi, *Corros. Sci*., 52 (2010) 152.
45. H. M. Elabbasy, H. S. Gadow, *J. Mol. Liq*., 321 (2021) 114918.
46. A. S. Fouda, H. S. El-Desoky, M. A. Abdel-Galeil, D. Mansour, *SN Appl. Sci.,* 3 (2021) 287.
47. M. K. H. Movahedinia, M. Shahidi-Zandi, *Int. J. Electrochem. Sci.,* 16 (2021) 1